Dual Targeting Of Tumor Associated Macrophages And Immunosuppressive Granulocytic Myeloid-Derived Suppressor Cells Augments Pd-1 Blockade In Cholangiocarcinoma

Sumera Rizvi* [1], Emilien Loeuillard[1], Jingchun Yang[1], Rory Smoot[2], Haidong Dong[3], Gregory Gores[1]

[1]Gastroenterology and Hepatology, [2]Department of Surgery, [3]Department of Urology, Mayo Clinic, Rochester, United States

Background

Cholangiocarcinoma (CCA)

- Biliary tract malignancy with limited therapeutic options and dismal prognosis (*Rizvi et al., Nat Rev Clin Oncol 2018*)
- Desmoplastic tumor with abundant tumor immune microenvironment (TIME)
- Response rate to immune checkpoint blockade monotherapy less than 10%

PD-1/PD-L1 Immune Checkpoint Pathway

- Programmed death-1 (PD-1) and its ligand PD-L1 are important immune resistance mechanisms in tumor biology which limit T cell cytotoxicity
- Therapeutic targeting of the PD-1/PD-L1 pathway with blocking antibodies restores T cell cytotoxicity

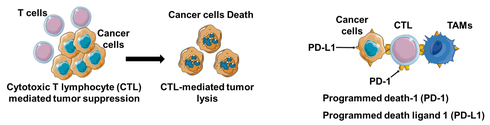

Limited T cell cytotoxicity as a mechanism of tolerance

Tumor Associated Macrophages (TAMs)

- Abundant in the TIME of CCA
- Potent source of PD-L1 and promote tumor progression by taming of adaptive immunity
- Activation of colony stimulating factor 1 receptor (CSF1R) by CSF1 secreted by cancer cells induces a pro-tumor macrophage phenotype

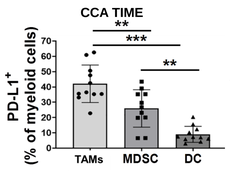

Tumor Associated Macrophages (TAMs)
Myeloid Derived Suppressor Cells (MDSC)
Dendritic Cells (DC)

Materials and Methods

- **Cell Lines**
  - Murine CCA cells (SB) derived from an oncogene-driven, genetic mouse model of CCA (*Yamada et al., Hepatology 2015)* express PD-L1

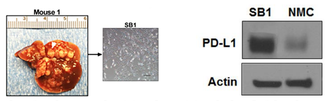

- **Syngeneic Orthotopic Murine Model of Cholangiocarcinoma with PD-L1 Expression**
  - C57BL/6 wild-type mice, Ccr2$^{-/-}$ mice
  - SB cells implanted orthotopically into mouse livers. Mice sacrificed 4 weeks after implantation

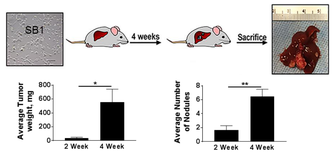

Figure 1

Recruited TAMs are the predominant source of PD-L1 in CCA

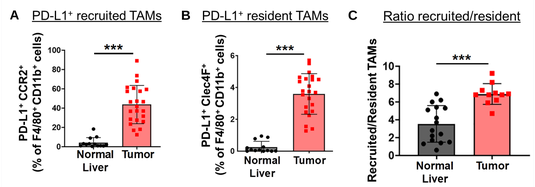

A. Percentage of PD-L1^{+} CCR2^{+} recruited TAMs in WT mouse liver or tumor 28 days after SB cells liver implantation, (n≥13). **B.** Percentage of PD-L1^{+} CCR2^{+} resident TAMs in WT mouse liver or tumor 28 days after SB cells liver implantation, (n≥13). **C.** Ratio of recruited TAMs (CD45^{+} CD11b^{+} F4/80^{+} CCR2^{+}) to resident TAMs (CD45^{+} CD11b^{+} F4/80^{+} Clec4F^{+}) in WT mouse liver (from mice without tumors) or SB tumor from WT mice, (n≥11). ***, *P*<.001

Figure 2

Ccr2$^{-/-}$ Mice Do Not Have a Reduction in CCA Tumor Burden

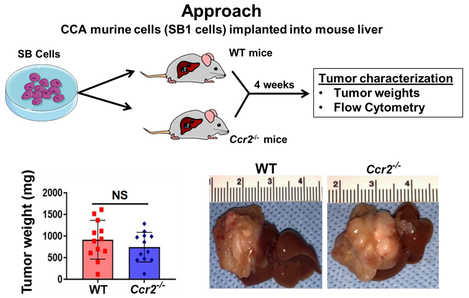

Average tumor weights in milligrams (mg) of wild type (WT) and *Ccr2*$^{-/-}$ mice 4 weeks following orthotopic implantation of SB cells and representative pictures of livers (n=12).

Figure 3

Depletion of Recruited Macrophages in *Ccr2*$^{-/-}$ mice Promote a Compensatory Infiltration of Granulocytic Myeloid-Derived Suppressor Cells (G-MDSCs)

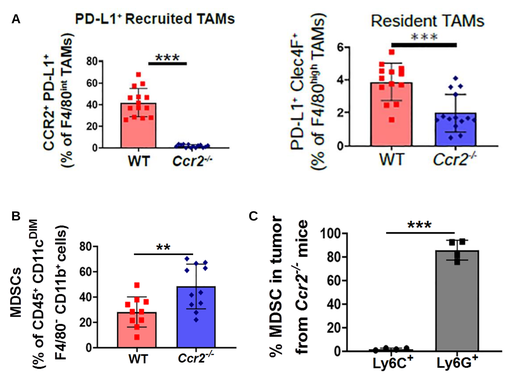

A. Using flow cytometry in WT and *Ccr2*$^{-/-}$ mouse tumors (4 weeks after SB cell implantation) expression of PD-L1 was analyzed on CCR2^{+} (left) or Clec4f^{+} (right) macrophages, (n≥12). **B.** Using flow cytometry in WT and *Ccr2*$^{-/-}$ mouse tumors (4 weeks after SB implantation) expression of Gr-1 was assessed in CD11c^{low} CD11b^{+} cells (n≥12). . **C.** Percentage of Ly6G^{+} and Ly6C^{+} MDSCs in *Ccr2*$^{-/-}$ mouse tumors, (n≥5). **, *P*<.01; ***, *P*<.001

Figure 4

Prevention of Macrophage Recruitment Promotes a Compensatory Infiltration of Granulocytic Myeloid-Derived Suppressor Cells (G-MDSCs)

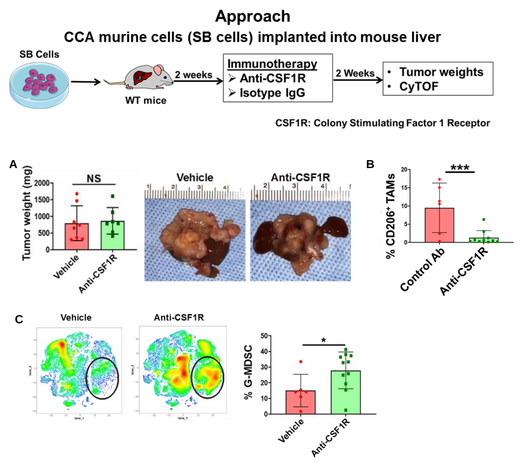

A. Average tumor weights in milligrams (mg) of WT mouse tumor and anti-CSF1R treated WT mouse tumor 4 weeks following SB implantation and representative pictures of livers. **B.** Percentage of CD206^{+} TAMs identify by CyTOF in WT mouse tumor and in anti-CSF1R treated WT mouse tumor 4 weeks following SB implantation. **C**. Mass cytometry (CyTOF) analysis of WT mouse tumors treated with vehicle or a colony stimulating factor 1 receptor (CSF1R) antibody for 2 weeks. Expression of unique clusters in mouse tumors visualized on a tSNE plot. Clusters were defined by panel of 24 cell surface markers. Representative tSNE plots (left) and percentage of G-MDSCs (right) in mice treated with vehicle or anti-CSF1R shown. Red indicates high frequency categorization of cells to a cluster; blue indicates low frequency. NS, non significant; *, *P*<.05; ***, *P*<.001

Figure 5

Accumulation of unique G-MDSC subsets induced by TAM blockade

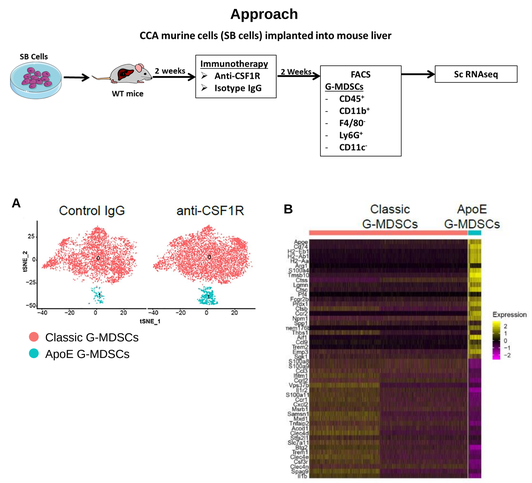

A. Cell clusters with similar expression profiles were further combined with resultant two distinct cell clusters. Percentage of cells in cluster classic G-MDSCs for control sample 98%, and 86% for anti-CSF1R sample. P value <0.01, Fisher's exact tast was used. **B.** Heatmap of gene expression profiles for selected top cluster specific gene (n=25 for cluster Classic G-MDSCs and cluster ApoE G-MDSCs, respectively). Expression values for each gene was z scored across all cells.

Figure 6

ApoE G-MDSCs are present in human CCA tumor immune microenvironment

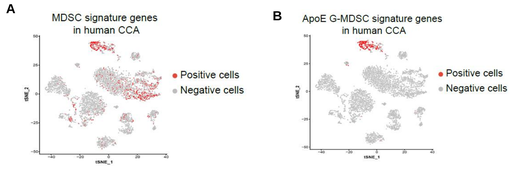

A. Enrichment analysis for a 40 signature human MDSCs gene using AUCell in human CCA (n=10). Significantly enriched cells are highlighted in red **B.** Enrichment analysis for 40 ApoE G-MDSCs signature genes using AUCell in human CA (n=10). Significantly enriched cells are highlighted in red.

Figure 7

Dual Inhibition of G-MDSCs and TAMs Potentiates Immune Checkpoint Blockade PD-1 in CCA

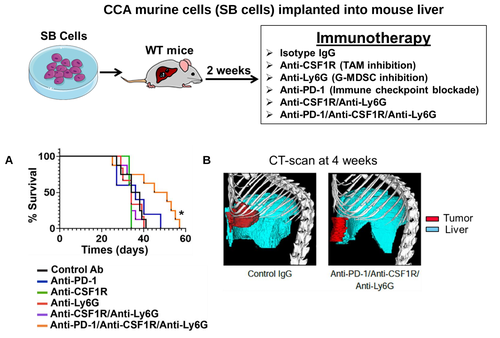

A. Survival curves in mice treated with control rat IgG isotype, anti-PD-1 (G4), anti-CSF1R (AFS98), anti-Ly6G (1A8), GW3965 alone or in the depicted combinations, (n≥5) **B**. Representative computed tomography image of liver tumor from a contrast reagent-injected mouse treated with control IgG isotype or anti-PD-1+anti-CSF1R+anti-Ly6G 28 days after implantation. The liver is depicted in blue color and the tumor in red. *, *P*<.05

Conclusions

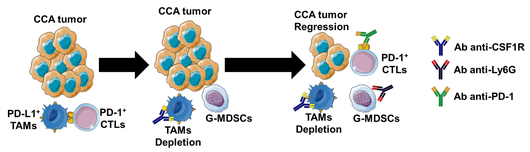

Dual blockade of G-MDSCs and TAMs potentiate anti-PD-1 therapy with a significant survival benefit in murine CCA and support the role of combinatorial therapeutic strategies.

Acknowledgments

NIH grant 1K08CA236874-01, AGA Research Scholar Award, Hepatobiliary SPORE Career Enhancement Award, Satter Foundation Liver Cancer Award, NIDDK-funded Mayo Clinic Center for Cell Signaling in Gastroenterology (P30DK084567), and the Mayo Foundation.

Rizvi Lab

Gores Lab

Haidong Dong, M.D., Ph.D.